Advances in Concrete Construction, *Vol. 3, No. 3 (2015) 237-250*
DOI: http://dx.doi.org/10.12989/acc.2015.3.3.237

SFRHPC interior beam-column-slab joints under reverse cyclic loading

N. Ganesan[a], M. Nidhi[*] and P.V. Indira[c]

Department of Civil Engineering, National Institute of Technology Calicut, Kerala, India

(Received September 30, 2015, Revised December 19, 2015, Accepted December 23, 2015)

Abstract. Beam-column joints are highly vulnerable locations which are to be designed for high ductility in order to take care of unexpected lateral forces such as wind and earthquake. Previous investigations reveal that the addition of steel fibres to concrete improves its ductility significantly. Also, due to presence of slab the strength and ductility of the beam increases considerably and ignoring the effect of slab can lead to underestimation of beam capacity and defiance of strong column weak beam concept. The influence of addition of steel fibres on the strength and behaviour of steel fibre reinforced high performance concrete (SFRHPC) interior beam-column-slab joints was investigated experimentally. The specimens were subjected to reverse cyclic loading. The variable considered was the volume fraction of crimped steel fibres i.e., 0%, 0.5% and 1.0%. The results show that the addition of steel fibres improves the first crack load, strength, ductility, energy absorption capacity and initial stiffness of the beam.

Keywords: beam-column-slab joint; energy absorption capacity; high performance concrete; high performance steel fibre reinforced cement concrete; reverse cyclic loading; stiffness degradation

1. Introduction

Beam-column joints, defined as that portion of the column within the depth of the deepest beam that frames into the column (ACI 352R-02, 2002) are the most susceptible locations in a reinforced concrete frame. When an unforeseen loading due to wind and earthquake acts on a structure, reversal of forces occur resulting in alternate compression and tension along the diagonals of the joint. This will create major distress in the joint region. Beam-column connections have an important role in the structural integrity of buildings and hence, they must be provided with adequate strength, stiffness and ductility to withstand the high intensity of loads transmitted to it. Owing to the importance of the behaviour of reinforced concrete (RC) beam-column joints subjected to seismic loading, several experimental investigations have been conducted by various researchers (Hanson and Conner1967, Ha and Cho 2008, Kim *et al.* 2009, Joyklad *et al.* 2012, Ganesan *et al.* 2013a, Rajagopal *et al.* 2014, Li *et al.* 2015)

∗Corresponding author, Ph.D. Student, E-mail: nidhi.srijith2012@gmail.com
[a]Professor, E-mail: ganesan@nitc.ac.in
[b]Professor, E-mail: indira@nitc.ac.in

http://www.techno-press.org/?journal=acc&subpage=7 ISSN: 2234-0912 (Print), 2234-179X (Online)

In most of the previous studies, the contribution of the slab is not explicitly considered. However, in a real RC building, the slab is monolithically cast with the beam and there is significant influence of the slab on the behaviour of RC beam-column joint. Since the interaction of the slab with the beams can significantly increase the flexural resistance of beam, ignoring the effect of the slab can lead to underestimation of beam capacity and violation of strong column-weak beam philosophy. However, a few studies on the effect of the slab in normal strength beam-column joints were carried out (Ehsani and Wight 1985, Durrani and Wight 1987, Pantazopoulou and French 2001, Shin and LaFave 2004, Canbolat and Wight 2008). Also, the addition of short discrete fibres to concrete have proved to enhance many engineering properties such as strength, ductility, stiffness (Naaman and Reinhardt 2004, Ganesan *et al.* 2013b, Ganesan *et al.* 2014a, Ganesan *et al.* 2014c). Moreover, the hybrid fibre reinforced concrete shows further improvement in these properties (Sukontasukkul 2004, Bajaj *et al*. 2012, Yan *et al.* 2012, Ganesan *et al.* 2013c).

However, investigations on steel fibre reinforced beam-column-slab joints have not yet been reported. Hence, an attempt was made to investigate the strength and performance of SFRHPC specimens subjected to reverse cyclic loading.

2. Research significance

Many of the works reported in the literature on seismic behaviour of reinforced concrete beam-column joints suggest the addition of fibres as a suitable method to enhance the ductility of beam-column joints (Ganesan *et al.* 2007, Priti *et al.* 2013, Abbas *et al.* 2014). Steel fibre reinforced high performance concrete (SFRHPC) in the joint region could improve the seismic behaviour of the joint region. However, these experimental works are based on skeletal beam-column joints. Only limited works have been carried out on beam-column-slab sub-assemblages. The effect of the slab on the behaviour of joints is significant especially when the slab participates in tension. In this experimental investigation, the effect of steel fibres on the strength and overall behaviour of interior HPC beam-column-slab joints are studied.

3. Experimental programme

The experimental investigation consisted of casting and testing of interior beam-column joints with slab subjected to reverse cyclic loading. Three numbers of 1/3rd scaled down beam-column slab joints were cast and tested to investigate the effect of different volume fractions of steel fibres in the general behaviour of the specimens.

3.1 Materials characterisation

The materials used consist of the following:

a) Portland Pozzolana Cement conforming to IS 1489 (Part 1):1991
b) Crushed stone fine aggregate passing through 4.75 mm IS sieve conforming to grading zone II of IS: 383-1970 (reaffirmed 2002) having fineness modulus 2.92 and specific gravity 2.39
c) Coarse aggregate with a maximum size 12.5 mm with specific gravity 2.78.

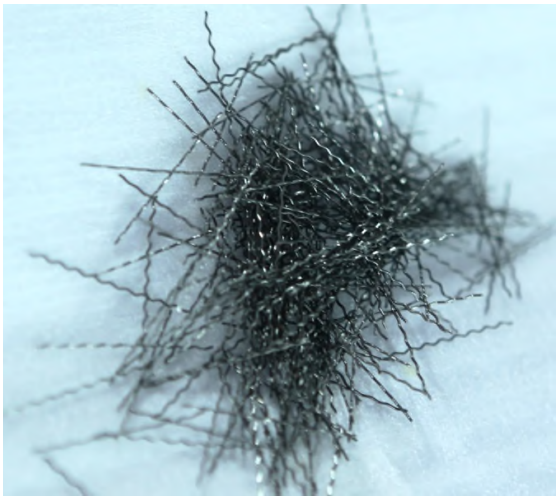

Fig. 1 Crimped steel fibres

d) Silica fume used as mineral admixtures
e) Crimped steel fibres of aspect ratio 66
f) Conplast SP430, a naphthalene based super-plasticizer was used for attaining workability.

The properties of silica fume and steel fibres used are given in Table 1 and Table 2 respectively. Fig. 1 shows the crimped steel fibres used in this study.

Table 1 Properties of silica fume

Specific gravity	2.10
SiO_2	90.36%
Moisture content	0.60%
Retained on 45 microns sieve	0.40%
Bulk Density	640 kg/ m^3

Table 2 Properties of steel fibre

Type	Crimped steel fibre
Length	30 mm
Diameter	0.45 mm
Aspect ratio	66
Ultimate tensile strength	800 MPa

M60 grade high performance concrete designed using ACI 211.1-91 (1991) procedure which was modified further by Aïtcin (1998) was used in this experimental investigation. Cement was partially replaced by micro filler silica fume. The required workability was attained by adjusting the superplaticizer dosage. The mix proportions used for the experimental investigation are given in Table 3.

Table 3 HPC mix proportions (kg/m3)

Cement	Silica fume	Fine aggregate	Coarse aggregate	Water	Super plasticizer
507	44	585	1059	149	22

3.2 Specimen details

In this experimental investigation three interior beam-column-slab connections were cast and tested. The beam of 150×200 mm cross section was reinforced with 10 mm diameter high yield strength deformed (HYSD) bars at top and bottom. The column having a cross section of 200×200 mm was reinforced with four 12 mm diameter HYSD bars. HYSD bars of 6 mm diameter were used as transverse reinforcement in columns and beams. Slab having a thickness of 60 mm was reinforced with 6 mm diameter HYSD bars at 190 mm spacing in both longitudinal and transverse directions. The mechanical properties of the reinforcements are given in Table 4 and the details of specimens in Table 5. Fig. 2 shows the overall dimension and details of reinforcement of interior beam-column-slab joint specimens.

Table 4 Mechanical properties of steel reinforcement

Diameter of bar (mm)	Yield strength (N/mm^2)	Ultimate strength (N/mm^2)	Modulus of elasticity (N/mm^2)
12	419	580	2.28×105
10	426	570	2.32×105
6	431	660	2.44×105

Table 5 Details of specimen

Sl. No	Designation	Volume fraction of fibres (%)
1	A1	0.0
2	A2	0.5
3	A3	1.0

3.3 Casting of specimens

The moulds for the specimens were fabricated using half-inch thick marine plywood. The reinforcement cage was placed in the mould correctly in position. Materials were batched by weight and mixed in the concrete mixer. Compaction of concrete within the mould was done using needle vibrator. The specimens were cast in the upright position in order to simulate actual construction practice. The specimens were cured for 28 days by using wet jute sacks which were wetted periodically to ensure continuous curing.

3.4 Test setup and instrumentation

The specimens were tested in a loading frame of 300 kN capacity. The top support of the column

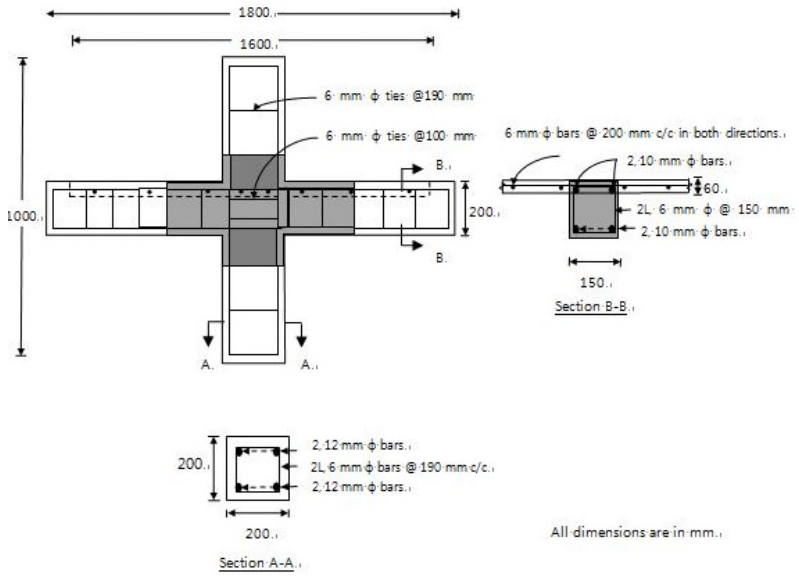

Fig. 2 Details of reinforcement beam-column-slab joint specimen

was a hinged support and the bottom of the column was firmly resting on top of the I-beam fixed to the test floor (Ganesan *et al.* 2013a, Ganesan *et al.* 2014b). The schematic illustration of the test arrangement and the photograph of the same are shown in Fig. 3 and Fig. 4 respectively. The specimens were subjected to reverse cyclic loading.

3.5 Loading sequence

The column axial load of 25% of the column capacity was applied by a hydraulic jack at column top and kept constant throughout the test. Reverse cyclic loading was applied at both the beam

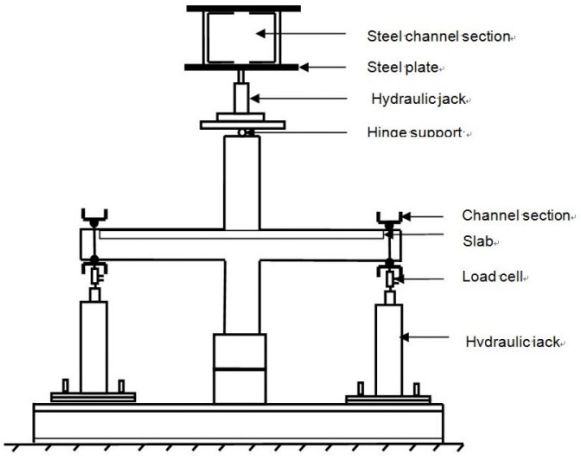

Fig. 3 Schematic diagram of test setup

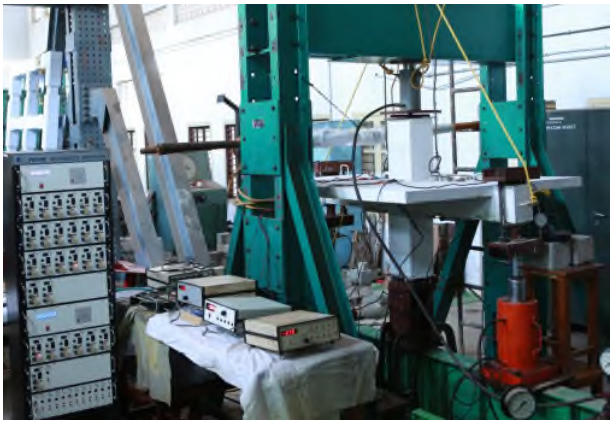

Fig. 4 Photograph of test arrangement

tips simultaneously in such a manner that when one beam is loaded in upward direction, the other one will be subjected to loading in downward direction and vice-versa. Typical loading sequence is given in Fig. 5.

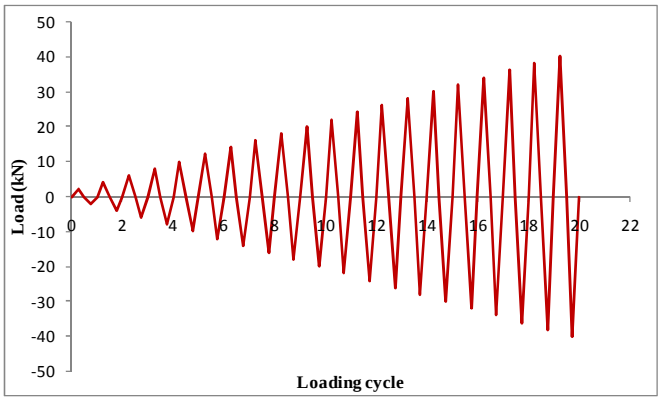

Fig. 5 Typical loading sequence

3.6 Overall behaviour of specimens

Figs. 6(a)-(c) shows the crack pattern observed in the specimens A1, A2 and A3 respectively. The first crack occurred in the soffit of the beam for all the specimens. The initial cracks propagated further during the successive loading cycles, leading to the formation of additional cracks in the beam portion. During the later stages of loading the cracks propagated from beam to the slab. Moreover, horizontal cracks parallel to the longitudinal reinforcement of the beam were observed on the top portion of the slab which deviated from the initial portion and branched out upon further loading as shown in Fig. 6(d). This indicates that the slab reinforcement effectively acts along with the longitudinal reinforcement of the beam when the slab is in tension and hence the effect of the slab should not be ignored. Also, as the volume fraction of fibres increased from 0

(a) HPC interior beam-column-slab joint (A1)

(b) SFRHPC interior beam-column-slab joint with 0.5% steel fibre (A2)

(c) SFRHPC interior beam-column-slab joint with 1.0% steel fibre (A3)

Fig. 6 Crack pattern of specimens A1, A2 and A3

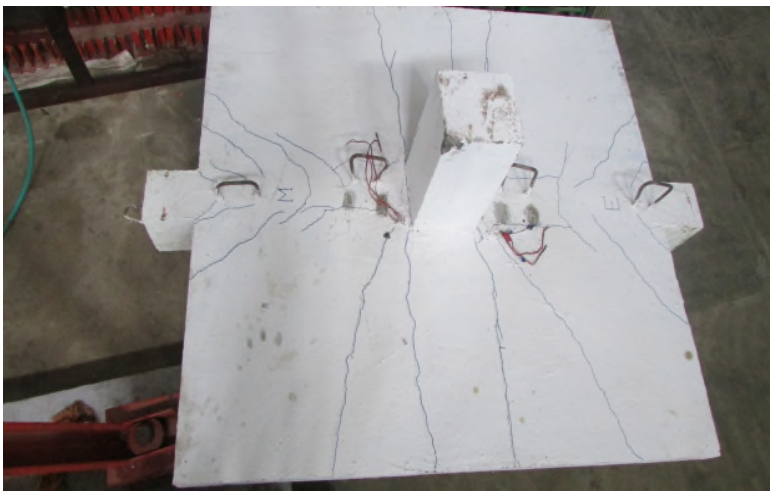

(d) Typical crack pattern on the slab

Fig. 6 Continued

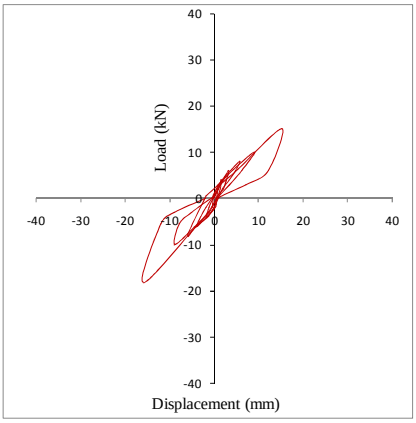

(a) HPC interior beam-column-slab joint (A1)

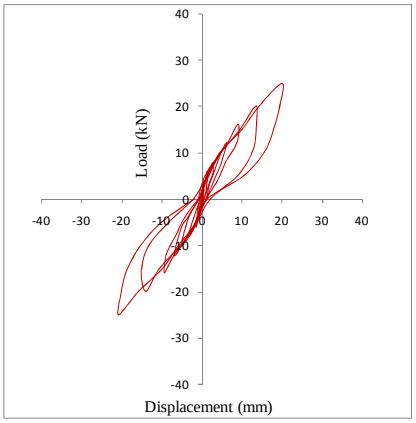

(b) SFRHPC interior beam-column-slab joint with 0.5% steel fibre (A2)

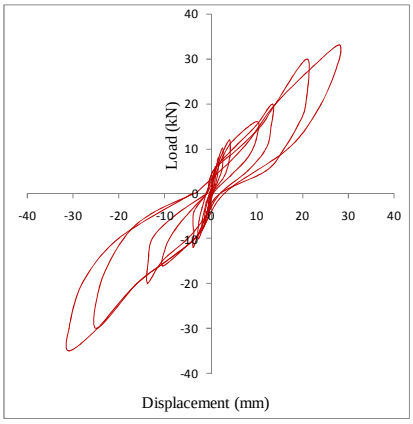

(c) SFRHPC interior beam-column-slab joint with 1.0 % steel fibre (A3)

Fig. 7 Typical load displacement plots of specimens A1, A2 and A3

to 0.5 % and 1.0 %, the load carrying capacity of the joint improved. This may be attributed to the fact that the crimped steel fibres intercepts the crack and prevents its further propagation. The cracks have to take a meandering path and hence more energy is dissipated during this process.

4. Test results and discussion

4.1 Load displacement behaviour

The load-displacement hysteresis loop gives a clear picture of the seismic performance of the structure. The typical load displacement plots of interior beam-column-slab joints A1, A2 and A3 subjected to reverse cyclic loading are given in Figs. 7(a)-(c). The peak or maximum value of the load-displacement plot was noted at each cycle of loading and the envelope of maximum load-displacement graph was plotted for each specimen by joining the peak load and displacement points at each cycle of loading and is shown in Fig. 8. The load corresponding to the point at which the envelope curve deviated from linearity is noted as the first crack load (Ganesan *et al.* 2014b). Table 6 shows the first crack load, ultimate load and displacement at ultimate load of the specimens.

SFRHPC beam-column-slab specimens with 0.5% and 1.0% of crimped steel fibres showed increase in load carrying capacity could undergo more cycles of loading and more displacement compared to the HPC specimen. It has been found that the first crack load increased by 54% for

Table 6 Test results

Designation of specimen	First crack load (kN)	Ultimate load (kN)		Displacement at ultimate load (mm)	
		Forward cycle	Reverse cycle	Forward cycle	Reverse cycle
A1	5.20	14.00	18.80	15.00	16.02
A2	8.00	25.00	28.00	18.99	20.76
A3	9.50	27.60	32.00	22.00	25.12

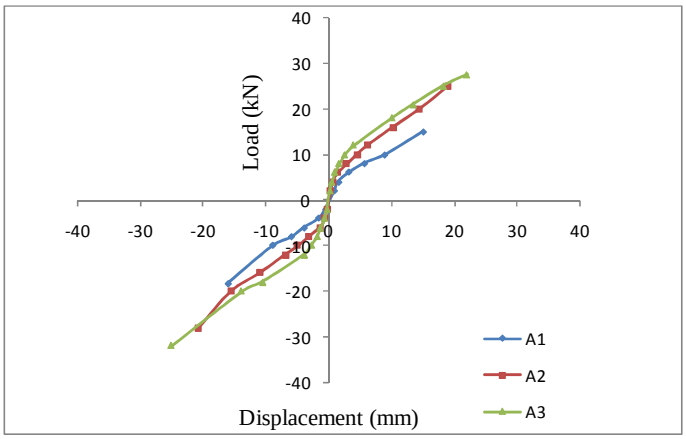

Fig. 8 Envelope of Load-displacement plots for specimens A1, A2 and A3

the SFRHPC specimen with 0.5% volume fraction of steel fibres and 83% for SFRHPC specimen with 1.0 % steel fibre when compared to HPC specimen. Addition of crimped steel fibres increases the tensile strain carrying capacity of concrete in the vicinity of the fibre and hence improves the first crack load and the ultimate load of the joints appreciably. When fibres are added to concrete, the overall properties of plain concrete will be modified due to the presence of fibres which try to intercept micro-level cracks, voids etc., in the plain concrete even before loading due to the compatibility between fibre and the matrix. The tensile strain of plain concrete in the neighbourhood of fibres would improve leading to enhanced cracking strength or modulus of rupture of the fibre concrete matrix. Because of these reasons Henagar and Doherty 1976; while formulating equations for flexure considered the tensile strength of concrete below neutral axis, while it is neglected in case of ordinary reinforced concrete. Hence, there is improvement in the first crack strength due to the presence of fibres. However, the quantum of increase depends on the volume fraction and orientation of fibres along with the bond efficiency factor.

An increase in ultimate load can be observed in the reverse cycle of loading in all the three specimens when compared to that in the forward cycle of loading. This may be due to the fact that the slab reinforcement within the effective width of the slab acts along with the longitudinal reinforcement of the beam when the slab is in tension and this contributes to the load carrying capacity of the joint.

4.2 Ductility characteristics

Ductility can be defined as the ability of a structure to undergo large inelastic deformations without significant reduction in its load carrying capacity. Enhancement to ductility, will lead to a better energy dissipation potential for the structural member. Displacement ductility factor is the ratio of ultimate displacement (δu) to the yield displacement (δy) which are obtained from the envelope load-displacement plot given in Fig. 8 (Paulay and Priestley 1992, Ganesan *et al.* 2014b). The displacement ductility factors were calculated and are given in Table 7. The displacement ductility factor for interior beam-column-slab specimens with 0.5% and 1% of crimped steel fibres are 1.18 times and 1.33 times higher than that of HPC specimen. Therefore, due to the addition of fibres, the ductility of specimens improves considerably.

Table 7 Displacement ductility factor

Designation of specimen	δ_y (mm)	δ_u (mm)	Displacement ductility factor	
			Absolute	Relative to HPC
A1	7.10	15.50	2.18	1.00
A2	7.70	19.88	2.58	1.18
A3	8.10	23.56	2.91	1.33

4.3 Energy dissipation capacity

During an earthquake, the structure absorbs energy which has to be dissipated gradually by inelastic rotations in the plastic hinge regions. Sudden dissipation of energy leads to a failure without ample warning leading to irreparable loss of life and structure. The energy dissipated by a

structural member can be calculated from the area enclosed within the load displacement hysteresis loop for each cycle of loading. The cumulative energy dissipated by the three specimens was calculated by summing up the energy dissipated in the successive load displacement loops throughout the test (Ganesan *et al.* 2014b). The cumulative energy dissipation of the specimens during each cycle is shown in Fig. 9. The cumulative energy dissipated is higher by 2.17 and 3.21 times for SFRHPC specimen with 0.5% and 1.0% steel fibre respectively when compared to HPC specimen. This implies that the SFRHPC specimens more ductile and give enough warning before failure when compared to HPC specimen.

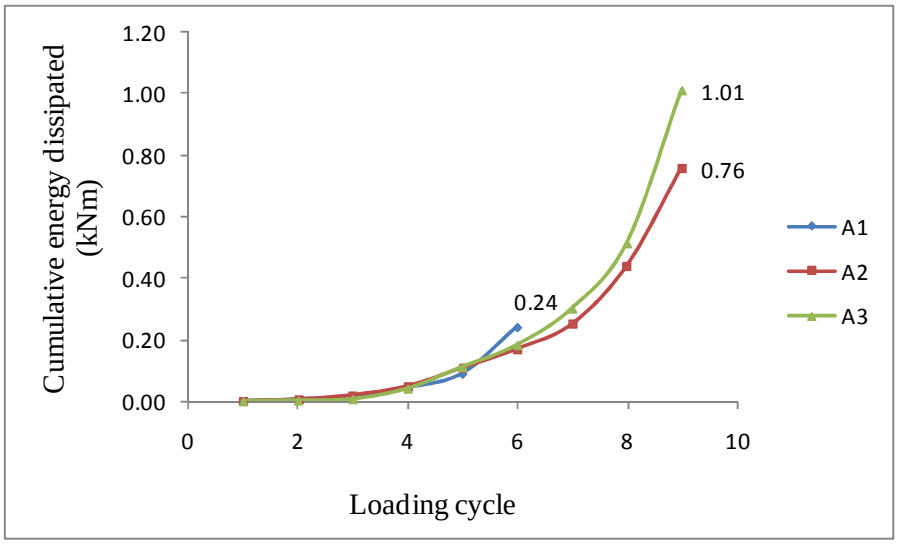

Fig. 9 Cumulative energy dissipation of specimens A1, A2 and A3

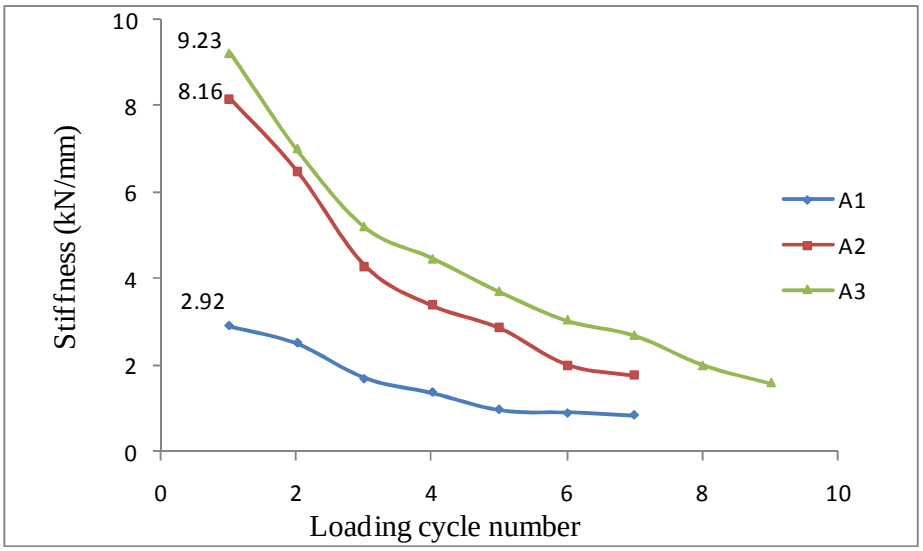

Fig. 10 Stiffness degradation plots of specimens A1, A2 and A3

4.4 Stiffness degradation

When subjected to several reversals of loadings RCC beam-column-joints will show stiffness degradation. Stiffness degradation is the result of cracking and loss of bond and the level of stiffness degradation depend upon the material properties and intensity of loading. The secant stiffness gives a measure of stiffness degradation and was calculated by drawing a line between the maximum positive displacement point in one half of the cycle and the maximum negative displacement point in the other half of the cycle (Paulay and Priestley 1992, Ganesan *et al.* 2014b) The stiffness degradation plots for the beam-column-slab joint specimens is shown in Fig. 10. It may be noted from the figure that as loading cycle increases, there is reduction in stiffness. The HPC specimen has lower initial secant stiffness than the SFRHPC specimens with 0.5% and 1.0% steel fibre. Also, as the number of cycles increases, the stiffness decreases, however, the SFRHPC specimens showed less stiffness degradation. This behaviour may be attributed to the following reason: as the number of cycles increase, microcracks develop and the steel fibres, which are distributed at random, intercept these cracks and bridge across these cracks. This controls further propagation of cracks and results in higher energy demand for debonding and pullout of steel fibres in the vicinity of cracks. During this process, stiffness of specimens with steel fibres will not undergo much reduction. The initial stiffness increased by 1.79 times and 2.16 times respectively for the SFRHPC specimen with 0.5% and 1.0% steel fibres when compared to that of HPC specimen.

4. Conclusions

Following are the conclusions obtained from this experimental investigation

- The SFRHPC beam-column-slab connection showed a considerable improvement in the in first-crack load, ultimate load, energy-dissipation capacity and ductility.
- The improvement of displacement ductility factor for SFRHPC specimen with 0.5% and 1.0 % steel fibre was 1.18 times and 1.33 times respectively when compared to the HPC specimen.
- In comparison with the HPC specimen, the cumulative energy dissipated for SFRHPC specimen with 0.5% and 1.0 % steel fibre respectively is higher by 2.17 and 3.21 times.
- The initial stiffness increased by 1.79 times and 2.16 times respectively for the SFRHPC specimen with 0.5% and 1.0 % steel fibres when compared to that of HPC specimen.
- The addition of steel fibres in HPC beam-column-slab joints improves many of the engineering properties such as load carrying capacity, ductility, energy absorption capacity of specimens to a greater extent and appears to be beneficial in the case of structures subjected to repeated or seismic loading.

References

Abbas, A.A., Mohsin, S.M.S. amd Cotsovos, D.M. (2014), "Seismic response of steel fibre reinforced concrete beam-column joints", *Eng. Struct.*, **59**, 261-283.

ACI 211.1-91 (1991), *Standard practice for selecting proportions for normal, heavyweight and mass concrete*, Farmington Hills: American Concrete Institute, USA.

ACI 352R-02 (Reapproved 2010), *Joint ACI-ASCE Committee 352 Report, Recommendations for design of*

beam-column connections in monolithic reinforced concrete structures, Farmington Hills: American Concrete Institute, USA.

Aïtcin, P.C. (1998), *High Performance Concrete*, E&FN Spon, London.

Bajaj, V., Singh, S.P., Singh, A.P. and Kaushik, S.K. (2012), "Flexural fatigue analysis of hybrid fibre-reinforced concrete", *Mag. Concrete Res.*, **64**(4), 361-373.

Canbolat, B.B. and Wight, J.K. (2008), "Experimental investigation on seismic behaviour of eccentric reinforced concrete beam-column-slab connections", *ACI Struct. J.*, **105**(2), 154-162.

Durrani, A.J. and Wight, J.K. (1987), "Earthquake resistance of connections including slabs", *ACI Struct. J.*, **85**(5), 400-406.

Ehsani, M. and Wight, J.K. (1985), "Effect of transverse beams and slab on beam-to-column connections", *ACI J.*, **82**(2), 188-195.

Ganesan, N., Bharati, R. and Shashikala, A.P. (2013a), "Behavior of self-consolidating rubberized concrete beam-column joints", *ACI Mater. J.*, **110**(64), 697-704.

Ganesan, N., Indira, P.V. and Anjana, S. (2013b), "Engineering properties of steel fibre reinforced geopolymer concrete", *Adv. Concrete Constr.*, **1**(4), 305-318.

Ganesan, N., Indira, P.V. and Anjana, S. (2014a), "Bond behaviour of reinforcing bars embedded in steel fibre reinforced geopolymer concrete", *Mag. Concrete Res.*, **67**(1), 9-16.

Ganesan, N., Indira, P.V. and Ruby, A. (2007), "Steel fibre reinforced high performance concrete beam-column joints subjected to cyclic loading", *ISET J Earthq Technol*, **44**, 445-456.

Ganesan, N., Indira, P.V. and Sabeena, M.V. (2013c), "Tension stiffening and cracking of hybrid fiber-reinforced concrete", *ACI Mater. J.*, **110**(66), 715-722.

Ganesan, N., Indira, P.V. and Sabeena, M.V. (2014b), "Behaviour of hybrid fibre reinforced concrete beam-column joints under reverse cyclic loads", *Mater. Des.*, **54**, 686-693

Ganesan, N., Indira, P.V. and Seena, P. (2014c), "High performance fibre reinforced cement concrete slender structural walls", *Adv. Concrete Constr.*, **2**(4), 309-324.

Ha,G.J. and Cho, C.G. (2008), "Strengthening of reinforced high-strength concrete beam–column joints using advanced reinforcement details", *Mag. Concrete Res.*, **60**(7), 487-497.

Hanson, N.W. and Conner, H.W. (1967), "Seismic resistance of reinforced concrete beam-column joints", *Proceedings ASCE*, **93**, 533-560.

Henager, C.H. and Doherty, T.J. (1976), "Analysis of reinforced fibrous concrete beams", *J. Struct. Dv.*, **102**(1), 177-188.

IS 1489 (Part I) (1991), Portland pozzolona cement specifications, Part I, Fly ash based, Bureau of Indian Standards, New Delhi.

IS 383 (1970), Specification for coarse and fine aggregates from natural sources for concrete, Bureau of Indian Standards, New Delhi. (reaffirmed 2002)

Joyklad, P., Pimanmas, A. and Dhakal, R.P. (2012), "Cyclic performance of beam-column joints with extended column fixed at base. Part I: experimental investigation", *Mag. Concrete Res.*, **64**(9), 807-825.

Kim, J., LaFave, J.M. and Song, J. (2009), "Joint shear behaviour of reinforced concrete beam-column connections", *Mag. Concrete Res.*, **61**(92), 119-132.

Naaman, A.E. and Reinhardt, H.W. (2004), "High performance fiber reinforced cement composites HPFRCC-4", *Cement Concrete Compos.*, **26**, 757-759.

Li, B., Lam, E.S.S., Wu, B. and Wang, Y.Y. (2015), "Seismic behavior of reinforced concrete exterior beam-column joints strengthened by ferrocement composites", *Earthq. Struct.*, **9**(1), 223-256.

Pantazopoulou, S. and French, C.W. (2001), "Slab participation in practical earthquake design of reinforced concrete frames", *ACI Struct. J.*, **98**(4), 1-11.

Paulay, T. and Priestley, M.J.N. (1992), *Seismic Design of Reinforced Concrete and Masonry Buildings*, John Wiley & Sons, NewYork.

Priti, A.P., Atul, K.D. and Jatin, A.D. (2013), "Evaluation of RC and SFRC exterior beam-column joint under cyclic loading for reduction in lateral reinforcement of the joint region", *Mag. Concrete Res.*, **65**(7), 405-414.

Rajagopal, S., Prabavathy, S. and Kang, T.H.K. (2014), "Seismic behavior evaluation of exterior

beam-column joints with headed or hooked bars using nonlinear finite element analysis", *Earthq. Struct.*, **7**(5), 861-875.
Shin, M. and LaFave, J.M. (2004), "Reinforced concrete edge beam-column-slab connections subjected to earthquake loading", *Mag. Concrete Res.*, **55**(6), 273-291.
Sukontasukkul, P. (2004), "Tensile behaviour of hybrid fibre-reinforced concrete", *Adv. Cement Res.*, **16**(3), 115-122.
Yan, L., Xing, Y.M. and Li, J.J. (2012), "High-temperature mechanical properties and microscopic analysis of hybrid-fibre-reinforced high-performance concrete", *Mag. Concrete Res.*, **65**(3), 139-147.

CC